AIMS Mathematics, 10(9): 22053–22074.
DOI: 10.3934/math.2025981
Received: 06 July 2025
Revised: 28 August 2025
Accepted: 05 September 2025
Published: 22 September 2025

https://www.aimspress.com/journal/Math

Research article

Soliton dynamics and stability of the time-fractional higher-order nonlinear Schrödinger equation: Analytical solutions and modulational instability analysis

Kanza Noor and Jamshad Ahmad*

Department of Mathematics, Faculty of Science, University of Gujrat, Gujrat-50700, Pakistan

* **Correspondence:** Email: jamshadahmadm@gmail.com.

Abstract: The paper investigates the soliton dynamics and stability analysis of the time-fractional higher-order nonlinear Schrödinger equation. A Caputo time-fractional derivative is included in the time fractional higher-order nonlinear Schrödinger equation, along with dispersive higher-order and nonlinear terms, which allow us to describe wave propagation in arbitrarily complex nonlinear and dispersive media in greater detail. Through the use of the ϕ^6-model expansion method, a vast range of precise analytical soliton solutions is obtained, comprising nonlinear, regular, and singular periodic solitons. The effects of the fractional higher-order physical parameters on the amplitude, width, and nature of these solitons are systematically examined. Moreover, the modulational instability is studied through the use of linear stability analysis. Plots are given in order to explain the change in the form and stability behavior, and the evolution of the soliton solutions as the parameters vary.

Keywords: Schrödinger equation; ϕ^6-model expansion method; soliton solutions; stability analysis
Mathematics Subject Classification: 35Q55, 35B35, 35C08, 35A20, 34A34

1. Introduction

The nonlinear Schrödinger equation (NLSE) is an elementary model for the dynamics of slowly varying wave packets in nonlinear dispersive media. It appears in a wide variety of scientific and engineering fields, such as nonlinear optics, quantum field theory, plasma physics, and Bose–Einstein condensates [1,2]. The classical NLSE has progressively been generalized to include the incorporation of higher-order effects like third-order dispersion, self-steepening, and self-frequency shifting to produce higher-order NLSEs that better model ultra-short pulse transmission in optical fibers and other intricate nonlinear systems [3]. Concurrently, the application of fractional calculus to nonlinear evolution equations has attracted much attention, as it can describe the memory and hereditary behavior that is inherent in most physical systems [4]. The time-fractional NLSE (TFNLSE) involving a

Caputo fractional derivative is an effective tool for describing the anomalous dispersion and non-Markovian dynamics in complex media [5–7]. Several analytical techniques have been created to solve fractional and higher-order NLSEs, including the inverse scattering method, the Darboux transformation, the Hirota bilinear method, and expansion and ansatz-type techniques [8]. Of these, model extension techniques present a versatile and strong methodology for producing various families of exact solutions. Specifically, the ϕ^6-model expansion method, initially developed within the context of quantum field theory and spontaneous symmetry breaking, has been applied to NLSEs with great success to obtain many types of soliton solutions, such as kink, anti-kink, bright, dark, and singular profiles [9, 10]. Moreover, recent advances in nonlinear wave dynamics in fractional and higher-order theories have also been made by [11]. The inclusion of the effects of higher orders is significant in terms of analyzing the structure of solitons. Despite the advancements made in the field, the extension of the ϕ^6 expansion procedure to the time-fractional higher-order NLSE (TFHNLSE) is still an unexplored field. This discrepancy is important because the incorporation of the fractional time derivative with higher-order spatial nonlinearities produces a model that can reproduce more complex wave dynamics, such as long-range memory effects and ultrafast dispersive interactions.
The TFHNLSE is given by [12]:

$$i\frac{\partial^\beta \chi}{\partial t^\beta} + a_1\frac{\partial^2 \chi}{\partial x^2} + a_2\chi - a_3|\chi|^2\chi + i\epsilon\frac{\partial^3 \chi}{\partial x^3} + 6|\chi|^2\frac{\partial \chi}{\partial x} = 0, \tag{1.1}$$

where $\chi(x,t)$ denotes the complex envelope of the optical field, $\beta \in (0,1]$ is the fractional order of the Caputo time derivative, and a_1, a_2, a_3, and ϵ are real constants that characterize dispersion, gain/loss, nonlinearity, and higher-order dispersion, respectively. The term $\frac{\partial^\beta \chi}{\partial t^\beta}$ introduces memory-dependent temporal evolution, reflecting the subdiffusive nature of wave propagation in certain nonlinear optical media.

There are important physical ramifications when the fractional time derivative is incorporated into Schrödinger-type models. It makes it possible to model media in the context of optical fibers where the temporal response is influenced by previous interactions and is not instantaneous. This is particularly relevant for disordered or composite media, where scattering, absorption, or nonlinear relaxation phenomena occur at multiple time scales. By adjusting the fractional order β, one can tune the model to fit the empirical data more accurately than with the classical (integer-order) models. There are substantial mathematical challenges with the TFHNLSE. The nonlinearity, dispersiveness, and fractionality in time of the equation complicate the existence, uniqueness, and stability of the solutions. Furthermore, the presence of third-order dispersion and nonlinear derivative terms necessitates the use of sophisticated analytical and numerical techniques to construct solutions. Nonetheless, when fractional-order dynamics are involved, the TFHNLSE's rich structure makes it an excellent place to discover novel wave phenomena like shock formations, rogue waves, and soliton-like structures.

From an application perspective, designing sophisticated optical systems requires an understanding of how femtosecond pulses behave through the lens of the TFHNLSE. Because optical fibers show nonlinear responses at high intensities, particularly over short time scales, they are not the best linear media. Dispersion and other higher-order effects affect these nonlinearities, which show up as four-wave mixing, self-phase modulation, and cross-phase modulation [13, 14]. A more comprehensive theoretical framework for simulating these effects is offered by the TFHNLSE, which makes it possible to create more effective systems in terms of transmission, compression, and pulse shaping.

Comparison with recent literature

Given the importance of realistic physical systems, much attention has recently been focused on stochastic and noise-perturbed generalizations of the NLSE and its fractional variants. Gepreel, Shohib, and Alngar [15] considered an example of noise effects on the stochastic resonant NLSE by incorporating two numerical integration schemes, showing how stochastic perturbations can change the resonance conditions, destabilize solitons, and even produce new dynamical phenomena. For example, [16] used stochastic Strichartz estimates to establish well-posedness and derive blow-up criteria to investigate the effect of multiplicative noise on the fractional NLSE. More generally, in a stochastic setting, (3+1)-dimensional stochastic NLSE have been studied, and many solitonic phenomena such as bright, dark, combined, and singular solitons have been revealed in the noisy settings characteristic of fluid dynamics and optical systems [17]. Moreover, [18] has also obtained exact bright, dark, singular, W-shaped soliton solutions to the generalized derivative NLSE with multiplicative noise and a conformable derivative, which gives an insight into the nature of the noise-induced wave characteristics. These studies underscore how stochastic perturbations can profoundly affect solitons' dynamics, altering their stability, morphology, and propagation properties. Abbagari et al. [19] recently studied multi-hump soliton and rogue wave solutions using the advanced analytical technique on a coupled nonlinear Schrödinger system. Although their work is an important step forward in the understanding of the process that produces the complex nonlinear structures through coupling, we will aim to further our study by incorporating the results into a single fractional higher-order nonlinear Schrödinger-type equation. The enlargement of the system's size by introducing the fractional-order derivatives and higher-order dispersive terms allows us to describe the memory-dependent dynamics and ultrafast waves, which are ignored by the coupled models. This difference highlights the originality of our contribution and locates the present work as a logical continuation of previous efforts in nonlinear evolution equations. In the near past, [20] studied the perturbed Gerdjikov–Ivanov model in the quintic case with a modified extended mapping approach and discovered a wide set of soliton solutions. Despite the fact that they studied another model, our fractional-order work augments this thus-far-limited body of literature by generalizing deterministic higher-order perturbed models to the nonlocal and memory-dominant regimes. Conversely, whereas noise-driven models are used to underline the influence of time-dependent fluctuations, fractional-order models point to the characteristic properties of anomalous dispersion and long-range correlations widely encountered in the field of nonlinear optics. A combination of these views augments our perception of soliton's behavior in real-world settings where tropical, chaotic perturbations, and fractional attributes are presented jointly. This paper advances the principles of controlled wave propagation using time-fractional dynamics through these contributions and produces useful insights that may find applications in quantum fluids, nonlinear optics, and signal transmission systems. The approaches and findings of this paper provide broader mathematical foundations, which will allow the study of fractional higher-order evolution equations and their associated soliton dynamics in the future [21, 22].

Our goal in this work is to perform a mathematical and physical analysis of the TFHNLSE. We investigate the impact of the fractional-order β on wave propagation, examine the analytical and semi-analytical approaches to obtain exact or approximate solutions, and talk about the possible physical interpretations of the findings [23, 24]. By doing this, we advance our theoretical knowledge of fractional nonlinear wave equations to aid in the realistic modeling of ultrafast optical phenomena

in complex media. The motivation for this study is that we seek to resolve the current deficiencies in our analysis regarding the TFHNLSE via advanced model expansion techniques. Specifically, we stress the utilization of the ϕ^6-model expansion method to procure the TFHNLSE's precise solitary wave solutions' novel categories. An ample array of analytical resolutions, including bright, periodic, kink-type, and singular solitons, may be fashioned via this method, augmenting the equation's solution space. Furthermore, this investigation endeavors to explore how such factors impact wave mechanics, considering the consequences of the fractional order and higher-order nonlinear coefficients on the extent, contour, and development of these solitonic formations, yielding a deep understanding. In addition, modulational instability (MI) analysis of the model through a linear stability analysis is crucial to assessing its physical significance and stability under perturbations [25, 26].

1.1. Definition

1.1.1. Caputo time-fractional derivative

i. Conceptual introduction

Ordinary calculus, using integer-order derivatives such as $d^n f/dt^n$, is usually inapplicable to systems with memory and hereditary effects, like the dynamics of viscoelastic bodies or anomalous diffusion in multiphase media. The notion behind fractional calculus is the generalization of differentiation to a non-integer order. Among the definitions that exist, the Caputo derivative is the most appropriate one for use in initial value problems in time. This is due to the primary benefit associated with it, which is the possibility of using the initial conditions in their conventional and well-understood physical realization (the initial position or, equivalently, the initial velocity). This cannot be done in the case of the Riemann-Liouville derivative, its main competitor.

ii. Formal definition

The formal definition of the Caputo derivative is given in terms of a singular integral. Let $\alpha > 0$ be a positive real number with $n - 1 < \alpha \leq n$ and a given differentiable, at least, n-times. A Caputo fractional derivative of order α is therefore defined as:

$$ {}_0^C D_t^\alpha f(t) = {}_0 I_t^{n-\alpha} \left(\frac{d^n f(t)}{dt^n} \right), \tag{1.2} $$

where ${}_0 I_t^\mu$ denotes the Riemann-Liouville integral of order $\mu > 0$, defined as

$$ {}_0 I_t^\mu f(t) = \frac{1}{\Gamma(\mu)} \int 0^t \frac{f(\tau)}{(t-\tau)^{1-\mu}} d\tau. \tag{1.3} $$

Properties of the Caputo derivative:

- Linearity
$$ {}^C D_t^\alpha [af(t) + bg(t)] = a\, {}^C D_t^\alpha f(t) + b\, {}^C D_t^\alpha g(t). $$
- Laplace transform
$$ \mathcal{L}\left\{ {}^C D_t^\alpha f(t) \right\}(s) = s^\alpha F(s) - \sum_{k=0}^{n-1} s^{\alpha-1-k} f^{(k)}(0). $$
- Derivative of a constant
$$ {}^C D_t^\alpha C = 0. $$

- Integer-order consistency

$$^{C}D_t^m f(t) = \frac{d^m f(t)}{dt^m}, \quad m \in \mathbb{N}.$$

- Relation to Riemann-Liouville integral

$$^{C}D_t^\alpha f(t) = {}_0I_t^{n-\alpha}\left(\frac{d^n f(t)}{dt^n}\right), \quad n-1 < \alpha < n.$$

2. Summary of the method

Consider the following time-fractional higher-order nonlinear partial differential equation (PDE)

$$\Xi(D_t^\beta \chi, \chi_t, \chi_{xx}, \chi_{tt}, \chi_{xt}, \cdots) = 0, \tag{2.1}$$

where D_t^β is a uniform fractional derivative, $\chi(x,t)$ is an unknown wave function, and Ξ is a polynomial in $\chi(x,t)$ with partial derivatives containing the highest derivatives and non-linear terms.

by setting the fractional wave transformation

$$\chi(x,t) = X(\rho)e^{i\nu(\varrho_1 x + \varrho_2 \frac{t^\beta}{\beta})}, where \rho = \varrho_3 x + \varrho_4 \frac{t^\beta}{\beta}, \tag{2.2}$$

where $\varrho_1, \varrho_2, \varrho_3$, and ϱ_4 are arbitrary non-zero constants and $X(\rho)$ is the amplitude function. By putting Eq (2.2) into Eq (2.1), the following complex ordinary differential equation (ODE) of non-linear degree is obtained

$$\Theta(X, iX', X'', X^2, \cdots) = 0. \tag{2.3}$$

2.1. The ϕ^6-model expansion method

Step 1. The solution of Eq (2.3) is presumed to be the subsequent form:

$$X(\rho) = \sum_{i=0}^{2N} \sigma_i(\phi^i(\rho)), \tag{2.4}$$

where σ_i are constants to be determined and $\phi(\rho)$ satisfies

$$(\phi')^2 = h_6\phi^6(\rho) + h_4\phi^4(\rho) + h_2\phi^2(\rho) + h_0, \tag{2.5}$$

where $h_i, (i = 0, 2, 4, 6)$ are constant and $h_6 \neq 0$.

Step 2. Balancing the highest-order derivatives and the largest nonlinear terms in Eq (2.3), we have the value of positive integer N in Eq (2.4).

Step 3. It is well known that Eq (2.5) has the solution:

$$\phi = \frac{H(\rho)}{\sqrt{sH(\rho)^2 + t}}, \tag{2.6}$$

where $\sqrt{sH(\rho)^2 + t} > 0$, and $H(\rho)$ solves the Jacobian elliptic equation [27].

$$(H^{'})^2 = l_4 H(\rho)^4 + l_2 H(\rho)^2 + l_0, \tag{2.7}$$

where $l_i (i = 0, 2, 4)$ is the constant to be determined. This converts the model into a form that is solvable in terms of known elliptic functions. s and t are given by

$$\mathrm{s} = \frac{h_4 (l_2 - h_2)}{3l_0 l_4 - \left(l_2^2 - h_2^2\right)}, \mathrm{t} = \frac{3l_0 l_4}{3l_0 l_4 - \left(l_2^2 - h_2^2\right)}, \tag{2.8}$$

under the constraint conditions

$$3h_6 \left(3l_0 l_4 - \left(l_2^2 - h_2^2\right)\right)^2 + h_4^2 (l_2 - h_2)(9l_0 l_4 - (l_2 - h_2)(h_2 + 2l_2)) = 0, 3h_0 h_4 - \left(3l_0 l_4 - \left(l_2^2 - h_2^2\right)\right) = 0. \tag{2.9}$$

Step 4. Substitute the solution of Eq (2.5) along with Eq (2.6) in Eq (2.4). The strategic equations are easily found by gathering the identical power coefficients to zero.

(1) The Jacobian elliptic equation's solutions are:

1. If $l_0 = 1 - m^2, l_2 = 2m^2 - 1, l_4 = -m^2$, then $H(\rho) = cn(\rho, m)$.
2. If $l_0 = 1, l_2 = -(1 + m^2), l_4 = m^2$, then $V(\rho) = sn(\rho, m) orcd(\rho, m)$.
3. If $l_0 = -m^2, l_2 = 2m^2 - 1, l_4 = 1 - m^2$, then $H(\rho) = nc(\rho, m)$.
4. If $l_0 = m^2, l_2 = -(1 - m^2), l_4 = 1$, then $H(\rho) = ns(\rho, m) ordc(\rho, m)$.
5. If $l_0 = m^2 - 1, l_2 = 2 - m^2, l_4 = -1$, then $H(\rho) = dn(\rho, m)$.
6. If $l_0 = -1, l_2 = 2 - m^2, l_4 = -(1 - m^2)$, then $H(\rho) = nd(\rho, m)$.
7. If $l_0 = 1, l_2 = 2 - m^2, l_4 = 1 - m^2$, then $H(\rho) = sc(\rho, m)$.
8. If $l_0 = 1, l_2 = 2m^2 - 1, l_4 = -m^2(1 - m^2)$, then $H(\rho) = sd(\rho, m)$.
9. If $l_0 = 1 - m^2, l_2 = 2 - m^2, l_4 = 1$, then $H(\rho) = cs(\rho, m)$.
10. If $l_0 = -m^2(1 - m^2), l_2 = 2m^2 - 1, l_4 = 1$, then $H(\rho) = ds(\rho, m)$.
11. If $l_0 = \frac{(1 - m^2)}{4}, l_2 = \frac{(1 + m^2)}{4}, l_4 = \frac{(1 - m^2)}{4}$, then $H(\rho) = nc(\rho, m) \pm sc(\rho, m)$.
12. If $l_0 = \frac{(1 - m^2)}{4}, l_2 = \frac{(1 + m^2)}{2}, l_4 = \frac{-1}{4}$, then $H(\rho) = mcn(\rho, m) \pm dn(\rho, m)$.
13. If $l_0 = \frac{1}{4}, l_2 = \frac{(1 - 2m^2)}{2}, l_4 = \frac{(1 - m^2)}{4}$, then $H(\rho) = \frac{sn(\rho, m)}{1 \pm cn(\rho, m)}$.
14. If $l_0 = \frac{1}{4}, l_2 = \frac{(1 + m^2)}{2}, l_4 = \frac{(1 - m^2)^2}{4}$, then $H(\rho) = \frac{sn(\rho, m)}{cn(\rho, m) \pm dn(\rho, m)}$.

(2) The limits of the Jacobian elliptic equations' solutions are

1. If $m \to 0$, then $sn(\rho, m) = sin(\rho)$. 2. If $m \to 1$, then $sn(\rho, m) anh(\rho)$.
3. If $m \to 0$, then $cd(\rho, m) = cos(\rho)$. 4. If $m \to 1$, then $cd(\rho, m) = 1$.
5. If $m \to 0$, then $cn(\rho, m) = cos(\rho)$. 6. If $m \to 1$, then $cn(\rho, m) = sech(\rho)$.
7. If $m \to 0$, then $ns(\rho, m) = csc(\rho)$. 8. If $m \to 1$, then $ns(\rho, m) = coth(\rho)$.
9. If $m \to 0$, then $cs(\rho, m) = cot(\rho)$. 10. If $m \to 1$, then $cs(\rho, m) = csch(\rho)$.
11. If $m \to 0$, then $sc(\rho, m) an(\rho)$. 12. If $m \to 1$, then $sc(\rho, m) = sinh(\rho)$.
13. If $m \to 0$, then $sd(\rho, m) = sin(\rho)$. 14. If $m \to 1$, then $sd(\rho, m) = sinh(\rho$.
15. If $m \to 0$, then $nc(\rho, m) = sec(\rho)$. 16. If $m \to 1$, then $nc(\rho, m) = coshh(\rho)$.
17. If $m \to 0$, then $dn(\rho, m) = 1$. 18. If $m \to 1$, then $dn(\rho, m) = sech(\rho)$.
19. If $m \to 0$, then $ds(\rho, m) = csc(\rho)$. 20. If $m \to 1$, then $ds(\rho, m) = csch(\rho)$.

3. Extraction of solutions

3.1. The ϕ^6-model expansion method

Substitute Eq (2.2) in Eq (1.1) and then separate the real and imaginary components. After simplification, we have a nonlinear ODE

$$\begin{aligned} &-\left(\varepsilon\left(-\varrho_1-3\varrho_3\right)\varrho_1^2+\varepsilon\left(\varrho_1+2\varrho_3\right)\left(3\varrho_1+1\right)\varrho_3\varrho_1-\varrho_2-\varrho_4\right)X''(\rho)\\ &+X(\rho)\left(-\varepsilon\varrho_1^3+\varepsilon\varrho_3\left(3\varrho_1+1\right)\varrho_1^2+\varrho_2\right)-\left(\left(6\varepsilon\varrho_1-6\varepsilon\left(\varrho_1+\varrho_3\right)\right)X(\rho)^3\right)=0. \end{aligned} \tag{3.1}$$

Setting the derivative of highest-order and the highest-degree nonlinear term of Eq (3.1) in balance, substituting Eq (2.5) and putting it in Eq (3.1), and equating all coefficients of the same power of $X^j(\rho)[X'(\rho)^f](j=0,1\ldots 8, f=1,2)$ to zero, we derive a system of algebraic equations.
Solving this system yields the following results:

$$\begin{aligned} \sigma_0 &= \frac{\sqrt{-8h_2\left(\varepsilon\varrho_1\left(-2\varrho_3^2(3\varrho_1+1)+\varrho_3\varrho_1(2-3\varrho_1)+\varrho_1^2\right)+\varrho_4+\varrho_2\right)-\left(\varrho_1^2(\varepsilon\varrho_3-\varepsilon\varrho_1+3\varepsilon\varrho_3\varrho_1)\right)-\varrho_2}}{3\sqrt{2}\sqrt{\varepsilon\varrho_3}}, \sigma_1=0,\\ h_4 &= -\frac{\sigma_2\sqrt{\varepsilon\varrho_3}\sqrt{-8h_2\left(\varepsilon\varrho_1\left(-2\varrho_3^2(3\varrho_1+1)+\varrho_3\varrho_1(2-3\varrho_1)+\varrho_1^2\right)+\varrho_4+\varrho_2\right)-\left(\varrho_1^2(\varepsilon\varrho_3-\varepsilon\varrho_1+3\varepsilon\varrho_3\varrho_1)\right)-\varrho_2}}{2\sqrt{2}\left(\varepsilon\varrho_1\left(-2\varrho_3^2(3\varrho_1+1)+\varrho_3\varrho_1(2-3\varrho_1)+\varrho_1^2\right)+\varrho_4+\varrho_2\right)},\\ h_6 &= -\frac{3\varepsilon\varrho_3\sigma_2^2}{8\left(\varepsilon\varrho_1\left(-2\varrho_3^2(3\varrho_1+1)+\varrho_3\varrho_1(2-3\varrho_1)+\varrho_1^2\right)+\varrho_4+\varrho_2\right)},\\ h_0 &= -\sqrt{-8h_2\left(\varepsilon\varrho_1\left(-2\varrho_3^2(3\varrho_1+1)+\varrho_3\varrho_1(2-3\varrho_1)+\varrho_1^2\right)+\varrho_4+\varrho_2\right)-\left(\varrho_1^2(\varepsilon\varrho_3-\varepsilon\varrho_1+3\varepsilon\varrho_3\varrho_1)\right)-\varrho_2}\\ &\quad\frac{\left(-4h_2\left(\varepsilon\varrho_1\left(-2\varrho_3^2(3\varrho_1+1)+\varrho_3\varrho_1(2-3\varrho_1)+\varrho_1^2\right)+\varrho_4+\varrho_2\right)+\varrho_1^2(\varepsilon\varrho_3-\varepsilon\varrho_1+3\varepsilon\varrho_3\varrho_1)+\varrho_2\right)}{18\sqrt{2}\sigma_2\sqrt{\varepsilon\varrho_3}\left(\varepsilon\varrho_1\left(-2\varrho_3^2(3\varrho_1+1)+\varrho_3\varrho_1(2-3\varrho_1)+\varrho_1^2\right)+\varrho_4+\varrho_2\right)}. \end{aligned} \tag{3.2}$$

The solutions to the presented family can be constructed, and the Jacobian elliptic functions(JEFs) are selected among those offered in Sections (2.2) and (2.3).
1(a). If $l_0=1-m^2, l_2=2m^2-1, l_4=-m^2$ and $m\to 0$, then $H(\rho)=cn(\rho,m)=cos(\rho)$, and we have

$$\chi_{1,2}=\left(\frac{\sigma_2\cos^2(\rho)}{\frac{(-h_2-1)h_4\cos^2(\rho)}{h_2^2-1}+\frac{3h_4}{h_2^2-1}}+\sigma_0\right)e^{i\left(\frac{\varrho_2\ell^\beta}{\beta}+x\varrho_1\right)}, \tag{3.3}$$

and constraint conditions are $h_4^2(-h_2-1)(-((-h_2-1)(h_2-2)))+3h_6\left(h_2^2-1\right)^2=0$, and $h_2^2+3h_0h_4-1=0$.
1(b). If $l_0=1-m^2, l_2=2m^2-1, l_4=-m^2$, and $m\to 1$, then $H(\rho)=cn(\rho,m)=sech(\rho)$, and we have

$$\chi_{3,4}=\left(\frac{\left(h_2^2-1\right)\sigma_2}{(1-h_2)h_4}+\sigma_0\right)e^{i\left(\frac{\varrho_2\ell^\beta}{\beta}+x\varrho_1\right)}. \tag{3.4}$$

The constraint equations are $h_4^2(1-h_2)(-((1-h_2)(h_2+2)))+3h_6\left(h_2^2-1\right)^2=0, h_2^2+3h_0h_4-1=0$.
2(a). If $l_0=1, l_2=-(1+m^2), l_4=m^2$, and $m\to 0$, then $H(\rho)=sn(\rho,m)=sin(\rho)$, and we have

$$\chi_{5,6}=e^{i\left(\frac{\varrho_2\ell^\beta}{\beta}+x\varrho_1\right)}\left(\sigma_0+\frac{\sigma_2\sin^2(\xi)}{\frac{(-h_2-1)h_4\sin^2(\rho)}{h_2^2-1}+\frac{3h_4}{h_2^2-1}}\right), \tag{3.5}$$

along with the constraints $\left(h_2^2+3h_0h_4-1\right)=0, \left(h_4^2\left(-h_2-1\right)\left(-\left(\left(-h_2-1\right)\left(h_2-2\right)\right)\right)+3h_6\left(h_2^2-1\right)^2\right)=0$.
2(b). If $l_0=1, l_2=-(1+m^2), l_4=m^2$, and $m\to 1$, then $H(\rho)=cn(\rho,m)anh(\rho)$, and we have

$$\chi_{7,8}=e^{i\left(\frac{\varrho_2 t^\beta}{\beta}+x\varrho_1\right)}\left(\sigma_0+\frac{\sigma_2\tanh^2(\rho)}{\frac{(-h_2-2)h_4\tanh^2(\rho)}{h_2^2-1}+\frac{3h_4}{h_2^2-1}}\right), \tag{3.6}$$

along with the constraints $\left(h_2^2+3h_0h_4-7\right)=0, \left(h_4^2\left(-h_2-2\right)\left(9-\left(-h_2-2\right)\left(h_2-4\right)\right)+3h_6\left(h_2^2-1\right)^2\right)=0$.
3(a). If $l_0=-m^2, l_2=2m^2-1, l_4=1-m^2$, and $m\to 0$, then $H(\rho)=nc(\rho,m)=\sec(\rho)$, and we have

$$\chi_{9,10}=\left(\frac{\left(h_2^2-1\right)\sigma_2}{\left(-h_2-1\right)h_4}+\sigma_0\right)e^{i\left(\frac{\varrho_2 t^\beta}{\beta}+x\varrho_1\right)}, \tag{3.7}$$

$h_4^2\left(-h_2-1\right)\left(-\left(\left(-h_2-1\right)\left(h_2-2\right)\right)\right)+3h_6\left(h_2^2-1\right)^2=0, h_2^2+3h_0h_4-1=0$.
3(b). If $l_0=-m^2, l_2=2m^2-1, l_4=1-m^2$, and $m\to 1$, then $H(\rho)=nc(\rho,m)=\cosh(\rho)$, and we have

$$\chi_{11,12}=\left(\frac{\sigma_2\cosh^2(\rho)}{\frac{(1-h_2)h_4\cosh^2(\rho)}{h_2^2-1}-\frac{3h_4}{h_2^2-1}}+\sigma_0\right)e^{i\left(\frac{\varrho_2 t^\beta}{\beta}+x\varrho_1\right)}, \tag{3.8}$$

$h_4^2\left(1-h_2\right)\left(-\left(\left(1-h_2\right)\left(h_2+2\right)\right)\right)+3h_6\left(h_2^2-1\right)^2=0, h_2^2+3h_0h_4-1=0$.
4(a). If $l_0=m^2, l_2=-(1-m^2), l_4=1$, and $m\to 0$, then $H(\rho)=ns(\rho,m)ordc(\rho,m)$,

$$\chi_{13,14}=\left(\frac{\left(h_2^2-1\right)\sigma_2}{\left(-h_2-1\right)h_4}+\sigma_0\right)e^{i\left(\frac{\varrho_2 t^\beta}{\beta}+x\varrho_1\right)}, \tag{3.9}$$

where $h_4^2\left(-h_2-1\right)\left(-\left(\left(-h_2-1\right)\left(h_2-2\right)\right)\right)+3h_6\left(h_2^2-1\right)^2=0, h_2^2+3h_0h_4-1=0$.
4(b). If $l_0=m^2, l_2=-(1-m^2), l_4=1$, and $m\to 1$, then $H(\rho)=ns(\rho,m)ordc(\rho,m)$,

$$\chi_{15,16}=\left(\frac{\sigma_2\coth^2(\rho)}{\frac{(-h_2-2)h_4\coth^2(\rho)}{h_2^2-1}+\frac{3h_4}{h_2^2-1}}+\sigma_0\right)e^{i\left(\frac{\varrho_2 t^\beta}{\beta}+x\varrho_1\right)}, \tag{3.10}$$

where $s=\frac{h_4\left(-\frac{h_4^2}{4h_6}-\frac{2h_0h_6}{h_4}-2\right)}{\left(\frac{h_4^2}{4h_6}+\frac{2h_0h_6}{h_4}\right)^2-1}$ and $t=\frac{3}{\left(\frac{h_4^2}{4h_6}+\frac{2h_0h_6}{h_4}\right)^2-1}$, and the constraint equations are $3h_6\left(h_2^2-1\right)^2+\left(9-\left(-h_2-2\right)\left(h_2-4\right)\right)\left(-h_2-2\right)h_4^2=0, -h_2^2+3h_0h_4+1=0$.
5(a). If $l_0=m^2-1, l_2=2-m^2, l_4=-1$, and $m\to 0$, then $H(\rho)=dn(\rho,m)=1$ from Section 2.3.

$$\chi_{17,18}=\left(\frac{\sigma_2}{\frac{(2-h_2)h_4}{h_2^2-1}-\frac{3h_4}{h_2^2-1}}+\sigma_0\right)e^{i\left(\frac{\varrho_2 t^\beta}{\beta}+x\varrho_1\right)}, \tag{3.11}$$

along with the constraints $h_4^2\left(2-h_2\right)\left(9-\left(2-h_2\right)\left(h_2+4\right)\right)+3h_6\left(h_2^2-1\right)^2=0, h_2^2+3h_0h_4-7=0$.
5(b). If $l_0=m^2-1, l_2=2-m^2, l_4=-1$, and $m\to 1$, then $H(\rho)=dn(\rho,m)=sech(\rho)$,

$$\chi_{19,20}=\left(\frac{\sigma_2\coth^2(\rho)}{\frac{(-h_2-2)h_4\coth^2(\rho)}{h_2^2-1}+\frac{3h_4}{h_2^2-1}}+\sigma_0\right)e^{i\left(\frac{\varrho_2 t^\beta}{\beta}+x\varrho_1\right)}, \tag{3.12}$$

along with the constraints $h_4^2\left(-h_2-2\right)\left(9-\left(-h_2-2\right)\left(h_2-4\right)\right)+3h_6\left(h_2^2-1\right)^2=0, h_2^2+3h_0h_4-7=0$.
6(a). If $l_0=-1, l_2=2-k^2, l_4=-(1-k^2)$, and $m\to 0$, then $V(0\varrho)=nd(\rho,m)=1$,

$$\chi_{21,22}=\left(\frac{\sigma_2}{\frac{(2-h_2)h_4}{h_2^2-1}-\frac{3h_4}{h_2^2-1}}+\sigma_0\right)e^{i\left(\frac{\varrho_2 r^\beta}{\beta}+x\varrho_1\right)}, \tag{3.13}$$

where $h_4^2\left(2-h_2\right)\left(9-\left(2-h_2\right)\left(h_2+4\right)\right)+3h_6\left(h_2^2-1\right)^2=0, h_2^2+3h_0h_4-7=0$.
6(b). If $l_0=-1, l_2=2-m^2, l_4=-(1-m^2)$, and $m\to 1$, then $H(\rho)=nd(\rho,m)=sech(\rho)$,

$$\chi_{23,24}=\left(\frac{\sigma_2\text{sech}^2(\rho)}{\frac{(1-h_2)h_4\text{sech}^2(\rho)}{h_2^2-1}-\frac{3h_4}{h_2^2-1}}+\sigma_0\right)e^{i\left(\frac{\varrho_2 r^\beta}{\beta}+x\varrho_1\right)}, \tag{3.14}$$

where $h_4^2\left(1-h_2\right)\left(-\left(\left(1-h_2\right)\left(h_2+2\right)\right)\right)+3h_6\left(h_2^2-1\right)^2=0, h_2^2+3h_0h_4-1=0$.
7(a). If $l_0=1, l_2=2-m^2, l_4=1-m^2$, and $m\to 0$, then $H(\rho)=sc(\rho,k)an(\rho)$,

$$\chi_{25,26}=\left(\frac{\sigma_2\tan(\rho)}{\frac{(2-h_2)h_4\tan(\rho)}{h_2^2-1}+\frac{3h_4}{h_2^2-1}}+\sigma_0\right)e^{i\left(\frac{\varrho_2 r^\beta}{\beta}+x\varrho_1\right)}, \tag{3.15}$$

where $h_4^2\left(2-h_2\right)\left(9-\left(2-h_2\right)\left(h_2+4\right)\right)+3h_6\left(h_2^2-1\right)^2=0, h_2^2+3h_0h_4-7=0$.
7(b). If $l_0=1, l_2=2-m^2, l_4=1-m^2$, and $m\to 1$, then $H(\rho)=sc(\rho,m)=sinh(\rho)$,

$$\chi_{27,28}=\left(\frac{\sigma_2\sinh(\rho)}{\frac{(1-h_2)h_4\sinh(\rho)}{h_2^2-1}+\frac{3h_4}{h_2^2-1}}+\sigma_0\right)e^{i\left(\frac{\varrho_2 r^\beta}{\beta}+x\varrho_1\right)}, \tag{3.16}$$

where $h_4^2\left(1-h_2\right)\left(-\left(\left(1-h_2\right)\left(h_2+2\right)\right)\right)+3h_6\left(h_2^2-1\right)^2=0, h_2^2+3h_0h_4-1=0$.
8(a). If $l_0=1, l_2=2m^2-1, l_4=-m^2(1-m^2)$, and $m\to 1$, then $H(\rho)=sd(\rho,m)=sinh(\rho)$,

$$\chi_{29,30}=\left(\frac{\sigma_2\sinh(\rho)}{\frac{(1-h_2)h_4\sinh(\rho)}{h_2^2-1}-\frac{3h_4}{h_2^2-1}}+\sigma_0\right)e^{i\left(\frac{\varrho_2 r^\beta}{\beta}+x\varrho_1\right)}, \tag{3.17}$$

where $h_4^2\left(1-h_2\right)\left(-\left(\left(1-h_2\right)\left(h_2+2\right)\right)\right)+3h_6\left(h_2^2-1\right)^2=0, h_2^2+3h_0h_4-1=0$.
8(b). If $l_0=1, l_2=2m^2-1, l_4=-m^2(1-m^2)$, and $m\to 0$, then $H(\rho)=sd(\rho,m)=sin(\rho)$,

$$\chi_{31,32}=\left(\frac{\sigma_2\sin(\rho)}{\frac{(2-h_2)h_4\sin(\rho)}{h_2^2-1}-\frac{3h_4}{h_2^2-1}}+\sigma_0\right)e^{i\left(\frac{\varrho_2 r^\beta}{\beta}+x\varrho_1\right)}, \tag{3.18}$$

where $h_4^2\left(2-h_2\right)\left(9-\left(2-h_2\right)\left(h_2+4\right)\right)+3h_6\left(h_2^2-1\right)^2=0, h_2^2+3h_0h_4-7=0$.
9(a). If $l_0=1-m^2, l_2=2-m^2, l_4=1$, and $m\to 0$, then $H(\rho)=cs(\rho,m)=\cot(\rho)$,

$$\chi_{33,34}=\left(\frac{\sigma_2\cot(\rho)}{\frac{(2-h_2)h_4\cot(\rho)}{h_2^2-1}+\frac{3h_4}{h_2^2-1}}+\sigma_0\right)e^{i\left(\frac{\varrho_2 r^\beta}{\beta}+x\varrho_1\right)}, \tag{3.19}$$

where $h_4^2\left(2-h_2\right)\left(9-\left(2-h_2\right)\left(h_2+4\right)\right)+3h_6\left(h_2^2-1\right)^2=0, h_2^2+3h_0h_4-7=0$.
9(b). If $l_0=1-m^2, l_2=2-m^2, l_4=1$, and $m\to 1$, then $H(\rho)=cs(\rho,m)=\operatorname{csch}(\rho)$,

$$\chi_{35,36}=\left(\frac{\left(h_2^2-1\right)\sigma_2}{\left(1-h_2\right)h_4}+\sigma_0\right)e^{i\left(\frac{\varrho_2\rho^\beta}{\beta}+x\varrho_1\right)}, \tag{3.20}$$

where $h_4^2\left(1-h_2\right)\left(-\left(\left(1-h_2\right)\left(h_2+2\right)\right)\right)+3h_6\left(h_2^2-1\right)^2=0, h_2^2+3h_0h_4-1=0$.
10(a). If $l_0=-m^2(1-m^2), l_2=2m^2-1, l_4=1$, and $m\to 0$, then $H(\rho)=ds(\rho,m)=csc(\rho)$,

$$\chi_{37,38}=\left(\frac{\left(h_2^2-1\right)\sigma_2}{\left(-h_2-1\right)h_4}+\sigma_0\right)e^{i\left(\frac{\varrho_2\rho^\beta}{\beta}+x\varrho_1\right)}, \tag{3.21}$$

where $h_4^2\left(-h_2-1\right)\left(-\left(\left(-h_2-1\right)\left(h_2-2\right)\right)\right)+3h_6\left(h_2^2-1\right)^2=0, h_2^2+3h_0h_4-1=0$.
10(b). If $l_0=-k^2(1-m^2), l_2=2m^2-1, l_4=1$, and $m\to 1$, then $H(\rho)=ds(\rho,m)=csch(\rho)$,

$$\chi_{39,40}=\left(\frac{\left(h_2^2-1\right)\sigma_2}{\left(1-h_2\right)h_4}+\sigma_0\right)e^{i\left(\frac{\varrho_2\rho^\beta}{\beta}+x\varrho_1\right)}, \tag{3.22}$$

where $h_4^2\left(1-h_2\right)\left(-\left(\left(1-h_2\right)\left(h_2+2\right)\right)\right)+3h_6\left(h_2^2-1\right)^2=0, h_2^2+3h_0h_4-1=0$.
11(a). If $l_0=\dfrac{(1-m^2)}{4}, l_2=\dfrac{(1+m^2)}{2}$, and $l_4=\dfrac{(1-m^2)}{4}$, then $H(\rho)=nc(\rho,m)\pm sc(\rho,m)$,

$$\chi_{41,42}=e^{i\left(\frac{\varrho_2\rho^\beta}{\beta}+x\varrho_1\right)}\left(\frac{\sigma_2(\tan(\rho)+\sec(\rho))^2}{\frac{\left(\frac{1}{2}-h_2\right)h_4(\tan(\rho)+\sec(\rho))^2}{h_2^2-\frac{7}{16}}+\frac{3h_4}{4\left(h_2^2-\frac{7}{16}\right)}}+\sigma_0\right), \tag{3.23}$$

where $h_4^2\left(\frac{1}{2}-h_2\right)\left(-\left(\left(\frac{1}{2}-h_2\right)\left(h_2+1\right)\right)-\frac{9}{16}\right)+3h_6\left(h_2^2-\frac{7}{16}\right)^2=0, h_2^2+3h_0h_4-\frac{1}{16}=0$.
11(b). If $l_0=\dfrac{(1-m^2)}{4}, l_2=\dfrac{(1+m^2)}{2}$, and $l_4=\dfrac{(1-m^2)}{4}$, then $H(\rho)=nc(\rho,m)\pm sc(\rho,m)$,

$$\chi_{43,44}=e^{i\left(\frac{\varrho_2\rho^\beta}{\beta}+x\varrho_1\right)}\left(\frac{\sigma_2(\sinh(\rho)+\cosh(\rho))^2}{\frac{\left(\frac{1}{2}-h_2\right)h_4(\sinh(\rho)+\cosh(\rho))^2}{h_2^2-\frac{1}{16}}+\frac{3h_4}{4\left(h_2^2-\frac{1}{16}\right)}}+\sigma_0\right), \tag{3.24}$$

where $h_4^2\left(\frac{1}{2}-h_2\right)\left(\frac{9}{16}-\left(\frac{1}{2}-h_2\right)\left(h_2+1\right)\right)+3h_6\left(h_2^2-\frac{1}{16}\right)^2=0, h_2^2+3h_0h_4-\frac{7}{16}=0$.
12(a). If $l_0=\dfrac{(1-m^2)}{4}, l_2=\dfrac{(1+m^2)}{2}, l_4=\dfrac{-1}{4}$, and $m\to 0$, then $H(\rho)=mcn(\rho,m)\pm dn(\rho,m)$,

$$\chi_{45,46}=\left(\frac{\sigma_2(\cos(\rho)+1)^2}{\frac{\left(\frac{1}{2}-h_2\right)h_4(\cos(\rho)+1)^2}{h_2^2-\frac{7}{16}}+\frac{3h_4}{4\left(h_2^2-\frac{7}{16}\right)}}+\sigma_0\right)e^{i\left(\frac{\varrho_2\rho^\beta}{\beta}+x\varrho_1\right)}, \tag{3.25}$$

where $h_4^2\left(\frac{1}{2}-h_2\right)\left(-\left(\left(\frac{1}{2}-h_2\right)(h_2+1)\right)-\frac{9}{16}\right)+3h_6\left(h_2^2-\frac{7}{16}\right)^2=0, h_2^2+3h_0h_4-\frac{1}{16}=0.$

12(b). If $l_0=\dfrac{(1-m^2)}{4}, l_2=\dfrac{(1+m^2)}{2}, l_4=\dfrac{-1}{4}$, and $m\to 1$, then $s=H(\rho)=mcn(\rho,m)\pm dn(\rho,m)$,

$$\chi_{47,48}=\left(\frac{\left(h_2^2-1\right)\sigma_2}{(1-h_2)\,h_4}+\sigma_0\right)e^{i\left(\frac{\varrho_2\rho^\beta}{\beta}+x\varrho_1\right)}, \tag{3.26}$$

where $h_4^2\,(1-h_2)\,(-((1-h_2)\,(h_2+2)))+3h_6\left(h_2^2-1\right)^2=0, h_2^2+3h_0h_4-1=0.$

13(a). If $l_0=\dfrac{1}{4}, l_2=\dfrac{(1-2m^2)}{2}$, and $l_4=\dfrac{1}{4}$, then $H(\rho)=\dfrac{sn(\rho,m)}{1\pm cn(\rho,m)}$,

$$\chi_{49,50}=e^{i\left(\frac{\varrho_2\rho^\beta}{\beta}+x\varrho_1\right)}\left(\frac{\sigma_2\tanh(\rho)}{(\mathrm{sech}(\rho)+1)\left(\frac{\left(-h_2-\frac{1}{2}\right)h_4\tanh(\rho)}{\left(h_2^2-\frac{1}{16}\right)(\mathrm{sech}(\rho)+1)}+\frac{3h_4}{4\left(h_2^2-\frac{1}{16}\right)}\right)}+\sigma_0\right), \tag{3.27}$$

where $h_4^2\left(-h_2-\frac{1}{2}\right)\left(\frac{9}{16}-\left(-h_2-\frac{1}{2}\right)(h_2-1)\right)+3h_6\left(h_2^2-\frac{1}{16}\right)^2=0, h_2^2+3h_0h_4-\frac{7}{16}=0.$

13(b). If $l_0=\dfrac{1}{4}, l_2=\dfrac{(1-2m^2)}{2}$, and $l_4=\dfrac{1}{4}$, then $H(\rho)=\dfrac{sn(\rho,m)}{1\pm cn(\rho,m)}$,

$$\chi_{51,52}=e^{i\left(\frac{\varrho_2\rho^\beta}{\beta}+x\varrho_1\right)}\left(\frac{\sigma_2\sin(\rho)}{(\cos(\rho)+1)\left(\frac{\left(\frac{1}{2}-h_2\right)h_4\sin(\rho)}{\left(h_2^2-\frac{1}{16}\right)(\cos(\rho)+1)}+\frac{3h_4}{4\left(h_2^2-\frac{1}{16}\right)}\right)}+\sigma_0\right), \tag{3.28}$$

where $h_4^2\left(\frac{1}{2}-h_2\right)\left(\frac{9}{16}-\left(\frac{1}{2}-h_2\right)(h_2+1)\right)+3h_6\left(h_2^2-\frac{1}{16}\right)^2=0, h_2^2+3h_0h_4-\frac{7}{16}=0.$

14(a). If $l_0=\dfrac{1}{4}, l_2=\dfrac{(1+m^2)}{2}, l_4=\dfrac{(1-m^2)^2}{4}$, and $m=0$, then $H(\rho)=\dfrac{sn(\rho,m)}{cn(\rho,m)\pm dn(\rho,m)}$,

$$\chi_{53,54}=e^{i\left(\frac{\varrho_2\rho^\beta}{\beta}+x\varrho_1\right)}\left(\frac{\sigma_2\sin(\rho)}{(\cos(\rho)+1)\left(\frac{\left(\frac{1}{2}-h_2\right)h_4\sin(\rho)}{\left(h_2^2-\frac{1}{16}\right)(\cos(\rho)+1)}+\frac{3h_4}{4\left(h_2^2-\frac{1}{16}\right)}\right)}+\sigma_0\right), \tag{3.29}$$

where $h_4^2\left(\frac{1}{2}-h_2\right)\left(\frac{9}{16}-\left(\frac{1}{2}-h_2\right)(h_2+1)\right)+3h_6\left(h_2^2-\frac{1}{16}\right)^2=0, h_2^2+3h_0h_4-\frac{7}{16}=0.$

14(b). If $l_0=\dfrac{1}{4}, l_2=\dfrac{(1+m^2)}{2}, l_4=\dfrac{(1-m^2)^2}{4}$, and $m=1$, then $H(\rho)=\dfrac{sn(\rho,m)}{cn(\rho,m)\pm dn(\rho,m)}$,

$$\chi_{55,56}=\left(\frac{\sigma_2\sinh(\rho)}{2\left(\frac{(1-h_2)h_4\sinh(\rho)}{2\left(h_2^2-1\right)}+\frac{3h_4}{4\left(h_2^2-1\right)}\right)}+\sigma_0\right)e^{i\left(\frac{\varrho_2\rho^\beta}{\beta}+x\varrho_1\right)}, \tag{3.30}$$

where $h_4^2\,(1-h_2)\,(-((1-h_2)\,(h_2+2)))+3h_6\left(h_2^2-1\right)^2=0, h_2^2+3h_0h_4-1=0$, and

$$\sigma_0=\frac{\sqrt{\varrho_1^2\left(\varrho_1\left(\varepsilon-3\varepsilon\varrho_3\right)-\varepsilon\varrho_3\right)-8h_2\left(\varepsilon\varrho_1\left(\varrho_1^2+(2-3\varrho_1)\,\varrho_3\varrho_1-2\left(3\varrho_1+1\right)\varrho_3^2\right)+\varrho_2+\varrho_4\right)}-\varrho_2}{3\sqrt{2}\sqrt{\varepsilon\varrho_3}}.$$

4. Stability analysis

The stability analysis of the TFHNLSE is essential to assess the inherent reliability of the system's solutions under small perturbations. It plays a vital role across various physical domains, including quantum mechanics, nonlinear optics, and plasma wave dynamics. The introduction of fractional derivatives significantly influences the system by incorporating memory effects and nonlocal behavior. In particular, the order β of the Caputo fractional derivative controls the strength of anomalous dispersion, introducing long-range temporal correlations that directly alter the modulational instability and gain dynamics.

Assuming Eq (1.1) with $\beta = 1$ has the following steady-state solution

$$\chi = \left(P(x,t) + \sqrt{\lambda}\right) e^{i\lambda t}, \tag{4.1}$$

where λ is the normalized optical power. Substituting Eq (4.1) into Eq (1.1) and linearizing, we obtain:

$$(-3a_3\lambda + a_2 - \lambda)(P + P^*) + i\frac{\partial P}{\partial t} + 6i\varepsilon\frac{\partial P}{\partial x} + a_1\frac{\partial^2 P}{\partial x^2} + i\varepsilon\frac{\partial^3 P}{\partial x^3}, \tag{4.2}$$

where $*$ denotes the complex conjugate.

We consider perturbations of the form

$$\begin{aligned} P(x,t) &= p_1 e^{-i(\eta x - t\varpi)} + p_2 e^{i(\eta x - t\varpi)}, \\ P^*(x,t) &= p_1 e^{i(\eta x - t\varpi)} + p_2 e^{-i(\eta x - t\varpi)}, \end{aligned} \tag{4.3}$$

where η is the wavenumber, ϖ represents the perturbation frequency, and p_1, p_2 are the normalized amplitudes. By inserting Eq (4.3) into Eq (4.2) and separating coefficients, we obtain the following dispersion relation:

$$a_1^2\eta^4 + 2a_1\eta^2\lambda + 6a_1a_3\eta^2\lambda - 2a_1a_2\eta^2 - \varepsilon^2\eta^6 + 12\varepsilon^2\eta^4 - 36\varepsilon^2\eta^2 - 2\varepsilon\eta^3\varpi + 12\varepsilon\eta\varpi - \varpi^2. \tag{4.4}$$

Solving Eq (4.4) for ϖ yields

$$\varpi = \sqrt{a_1^2\eta^4 + 2a_1\eta^2\lambda + 6a_1a_3\eta^2\lambda - 2a_1a_2\eta^2} - \varepsilon\eta^3 + 6\varepsilon\eta. \tag{4.5}$$

If ϖ is bounded and real, the solution is stable. Instability arises when the square root becomes negative, producing a complex ϖ that indicates the growth of perturbations. A nonlinear contribution proportional to ε may either suppress or amplify this growth, depending on its sign.

In the case of $\beta \neq 1$, the time derivative of Eq (4.2) becomes fractional, which brings about nonlocal temporal memory and anomalous dispersion. In the frequency domain, this changes the term of frequency follows:

$$i\frac{\partial P}{\partial t} \quad \longrightarrow \quad (i\varpi)^\beta P,$$

and thus the dispersion relation is generalized as follow:

$$\varpi^\beta = a_1^2\eta^4 + 2a_1\eta^2\lambda + 6a_1a_3\eta^2\lambda - 2a_1a_2\eta^2 - \varepsilon^2\eta^6 + 12\varepsilon^2\eta^4 - 36\varepsilon^2\eta^2 - 2\varepsilon\eta^3\varpi + 12\varepsilon\eta\varpi.$$

This means that both growth rate and stability thresholds are highly affected by β. The memory enhances the stability region by slowing down perturbation growth, and prevents modulational instability, at least in the case of $\beta < 1$. The enhanced anomalous dispersion will be present at $\beta > 1$, can shift the gain peaks, and can cause the earlier onset of instability.
The gain instability expression is thus amended as follows:

$$G(\varpi;\beta) = \mathrm{Im}\left[(\varpi)^{\beta}\right] = \mathrm{Im}\left[\left(\sqrt{a_1^2\eta^4 + 2a_1\eta^2\lambda + 6a_1a_3\eta^2\lambda - 2a_1a_2\eta^2} - \varepsilon\eta^3 + 6\varepsilon\eta\right)^{\beta}\right]. \tag{4.6}$$

At an integral $\beta = 1$, this coincides with the classical gain spectrum, as in Eq (4.6). In the case of a fractional β, the spectral profile is changed dramatically, and more bandwidth or shifted instability bands emerge. Such fractional dependency offers direct physical control of modulational instability and control of rogue-wave generation in optical systems.

Comparison diagram of spatial distribution and temporal evolution with specified parameters as shown in Figure 1.

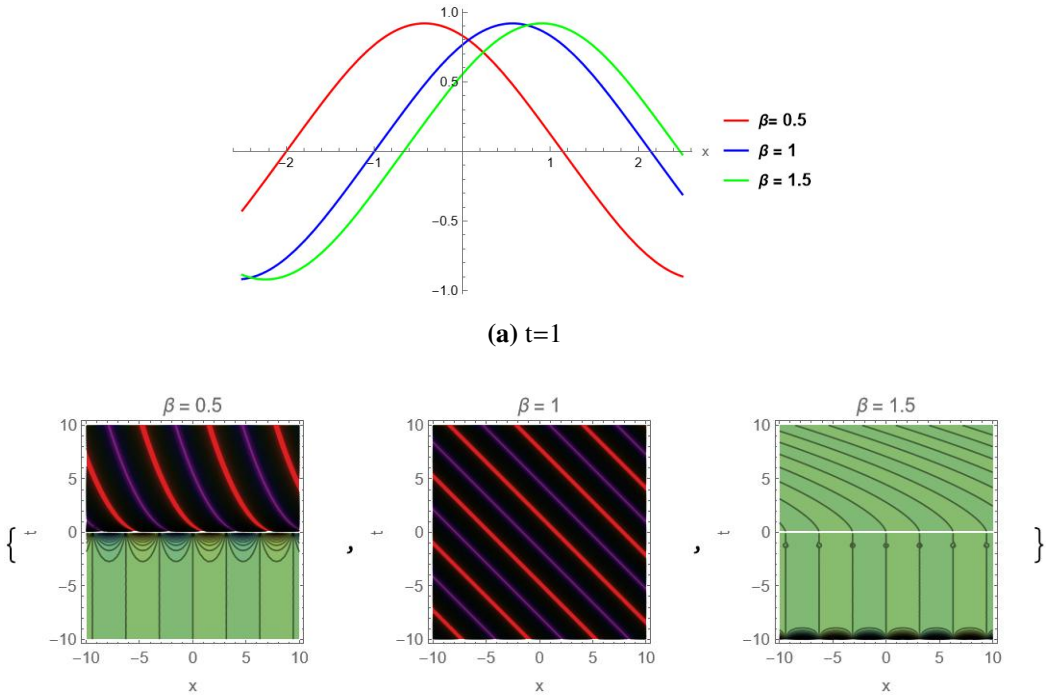

(a) t=1

(b)

Figure 1. Graphical illustration of the solution of Eq (3.3) for $h_4 = 1,\ \varepsilon = 1,\ h_2 = 0.4,\ h_6 = 0.2,\ h_0 = 0.1,\ \sigma_2 = 0.1,\ \varrho_3 = 1; \varrho_2 = 1,\ \varrho_1 = 1$, and $\varrho_4 = 1$.

Comparative analysis of spatial wave propagation and temporal evolution patterns demonstrating solution behavior under varying parameter conditions as shown in Figure 2.

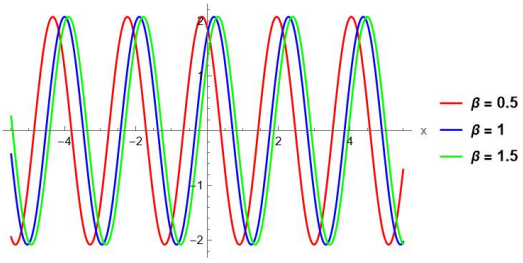

(a) t=1

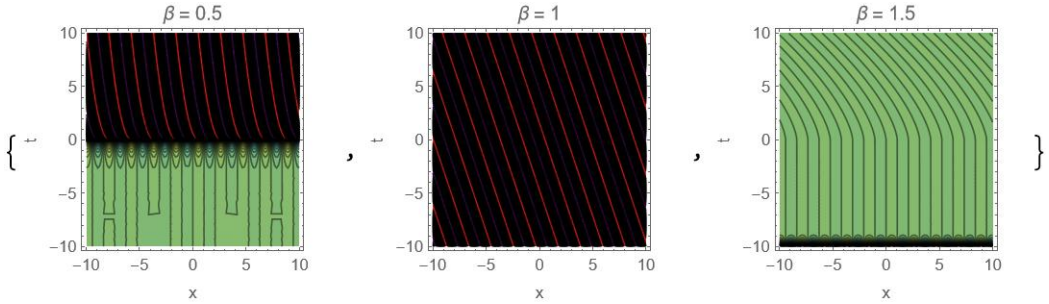

(b)

Figure 2. Graphical illustration of the solution of Eq (3.4) for $h_4 = 0.1; \varepsilon = 0.1; h_2 = 0.3; h_6 = 0.9; h_0 = 0.1; \sigma_2 = 0.1; \varrho_3 = 2; \varrho_2 = 1; \varrho_1 = 3; \varrho_4 = 9$.

Spatiotemporal evolution pattern demonstrating wave propagation characteristics as shown in Figure 3.

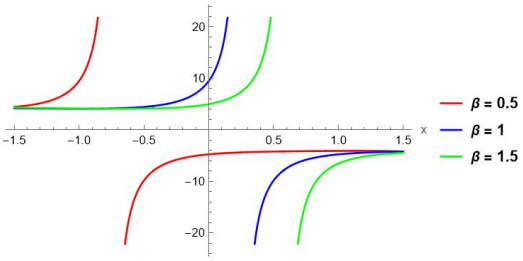

(a) t=1

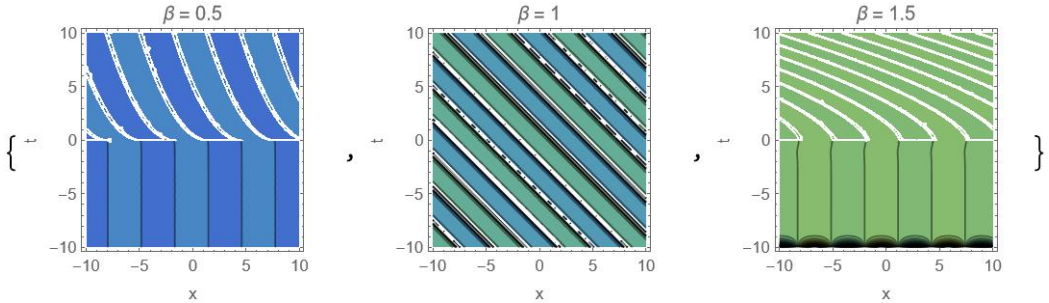

(b)

Figure 3. Graphical illustration of the solution of Eq (3.15) for $h_4 = 1; h_2 = 3; h_6 = 0.9; h_0 = 1; \sigma_2 = 1; \varrho_3 = 1; \varrho_2 = 1; \varrho_1 = 1; y = 1; \varepsilon = 0.1; z = 1; \varrho_4 = 1$.

Time space analysis illustrating solution characteristics under specified parameter conditions as shown in Figure 4.

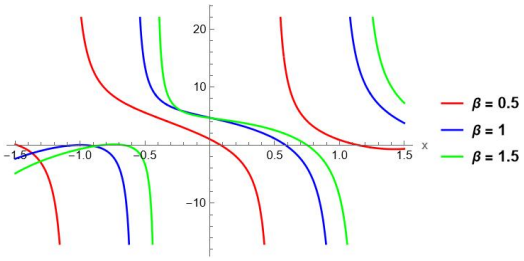

(a) t=1

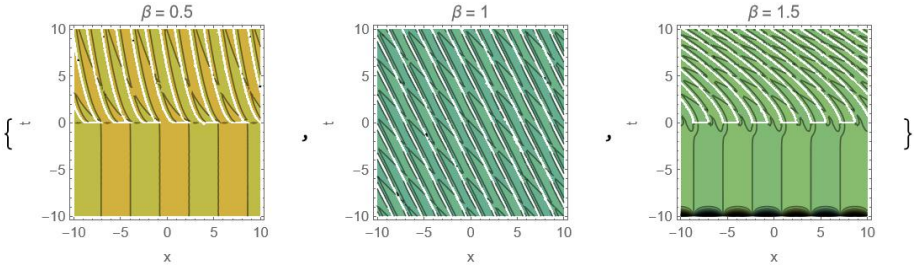

(b)

Figure 4. Graphical illustration of the solution of Eq (3.19) for $h_4 = 0.1; h_2 = 1.5; h_6 = 0.4; h_0 = 1; \sigma_2 = 1; \varrho_3 = 2; \varrho_2 = 1; \varrho_1 = 1; y = 1; \varepsilon = 1; z = 1; \varrho_4 = 1$.

Spatiotemporal solution dynamics demonstrating wave propagation characteristics as shown in Figure 5.

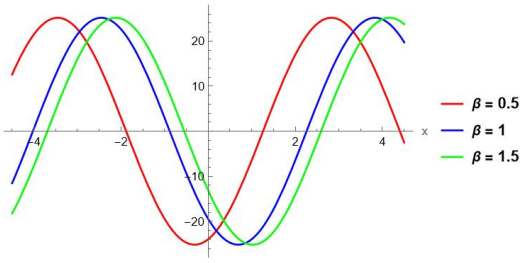

(a) t=1

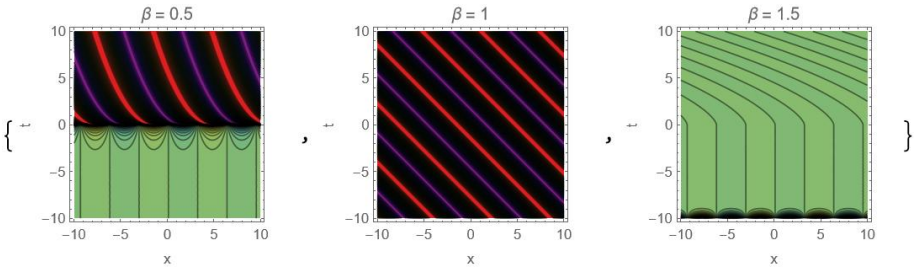

(b)

Figure 5. Graphical illustration of the solution of Eq (3.20) for $h_4 = 0.1; h_2 = 1.5; h_6 = 0.4; h_0 = 1; \sigma_2 = 1; \varrho_3 = 1; \varrho_2 = 1; \varrho_1 = 1; \varepsilon = 0.1; \varrho_4 = 1$.

Instantaneous spatial amplitude distribution contrasted with comprehensive temporal evolution pattern showing solution dynamics as shown in Figure 6.

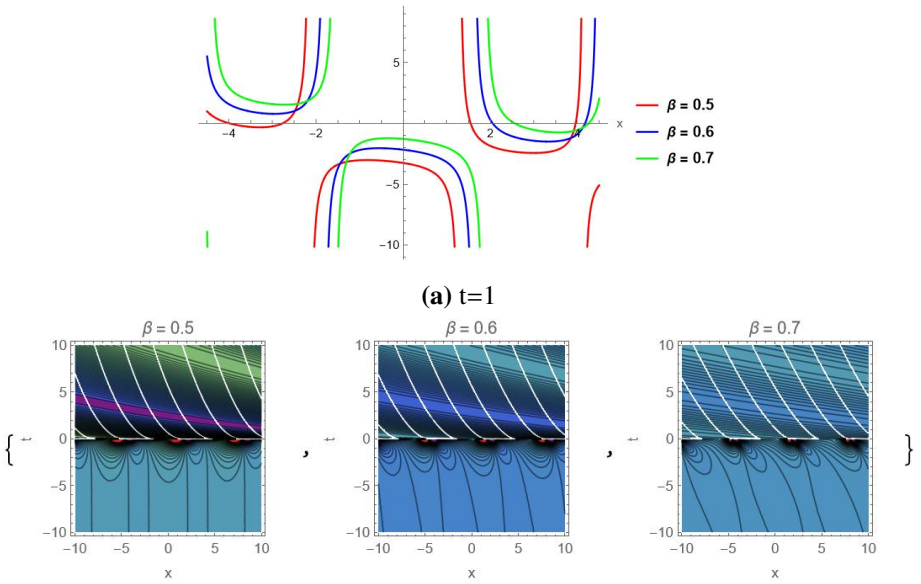

(a) t=1

(b)

Figure 6. Graphical illustration of the solution of Eq (3.23) for $h_2 = 1.5; h_4 = 1; \varepsilon = 0.1; h_6 = 0.4; h_0 = 1; \sigma_2 = 1; \varrho_3 = 1; t = 1; \varrho_2 = 1; \varrho_1 = 0.1; \varrho_4 = 1$.

Comparative behavior demonstrating wave propagation under modified parameter conditions as shown in Figure 7.

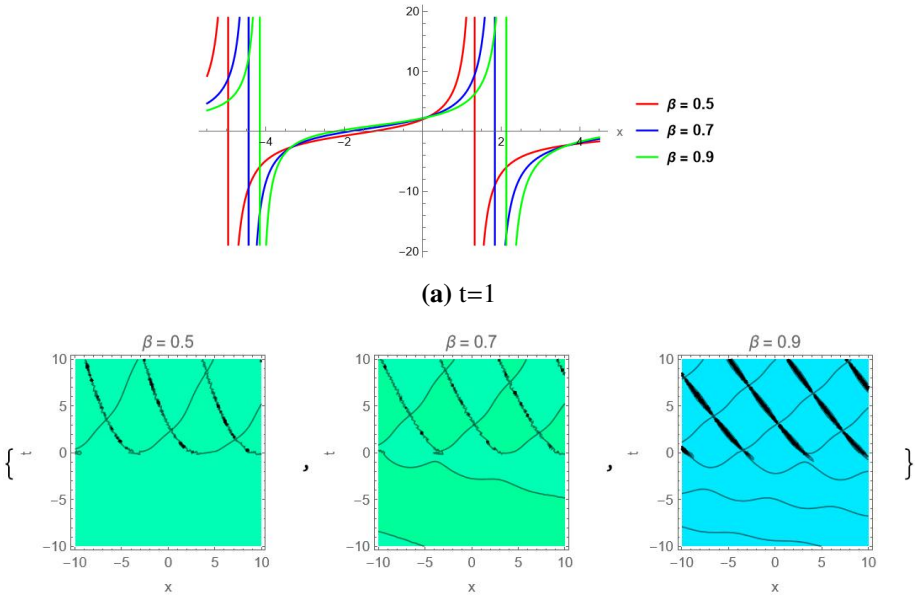

(a) t=1

(b)

Figure 7. Graphical illustration of the solution of Eq (3.28) for $h_2 = 0.5; h_4 = 0.1; h_6 = 0.4; h_0 = 0.1; \sigma_2 = 1; \varrho_3 = 1; \varrho_2 = 1; \varrho_1 = 0.1; \varepsilon = 0.1; \varrho_4 = 0.91$.

Comparative wave behavior demonstrating propagation characteristics for different parameter sets as shown in Figure 8.

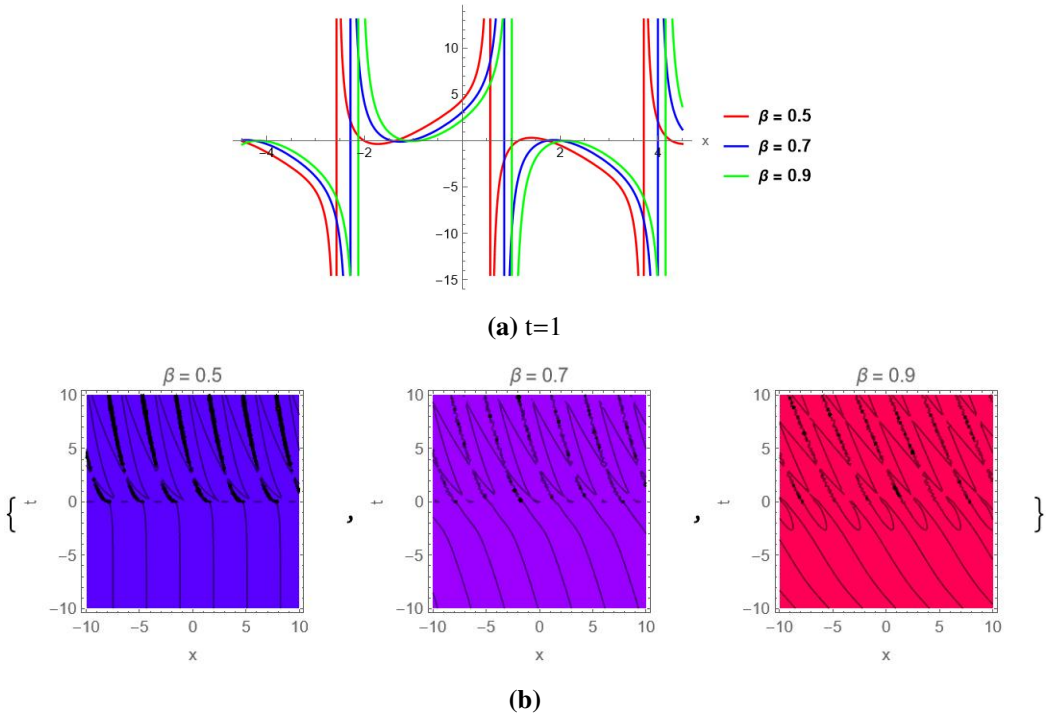

(a) t=1

(b)

Figure 8. Graphical illustration of the solution of Eq (3.29) for $h_2 = 0.5; h_4 = 0.1; h_6 = 0.4; h_0 = 0.1; \sigma_2 = 1; \varrho_3 = 2; \varrho_2 = 1; \varrho_1 = 1; \varrho_4 = 1; \varepsilon = 0.1$.

Stability region visualization across varying parameter sets as shown in Figure 9.

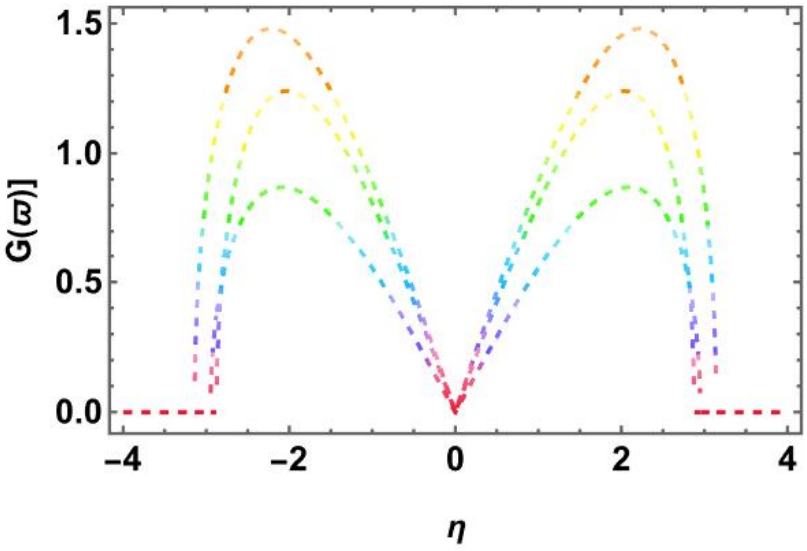

Figure 9. Graphical illustration of Eq (4.6) for $a_1 = \{0.2, 0.3, 0.4\}; \varepsilon = \{0.2, 0.25, 0.3\}; a_2 = \{1, 1.8, 1.9\}; \lambda = \{0.1, 0.2, 0.3\}; a_3 = \{0.1, 0.2, 0.4\}$.

5. Discussion

To see a visual representation of the solitons, we have used two-dimensional graphs of the soliton positions with respect to $t = 1$ and have also provided contour plots. Collectively, the 2D and contour diagrams depict a complete picture of the model parameters and demonstrate how the fractional order can be matched to control soliton propagation. Figure 1 shows the periodic soliton response that involves nonlinearity embedded in the TFHNLSE model with the localized and with the constraintsmodulated features of waves. The red graph represents a smaller value of h_2, exhibiting a thinner soliton distribution, whereas the blue graph represents a balanced average bell-shaped soliton. With larger values of h_2 and h_4, the green curve shows a compressed soliton. Figure 2 shows steady periodic oscillatory wave forms, as exhibited by nonlinear optical waveguides, photonic lattices, and Bose-Einstein condensates. By tuning the system's parameters, we can adapt the amplitude and frequency, so these solutions are applicable in the periodic pulse train design, multichannel carriers in fiber-optics, and ultrafast switching in dispersive media with memory effects. Figure 3 exhibits single-periodic dependence with the energies in the form of a tangent, and vertical asymptotes are observed at some discrete points in space. Both the steepness and the localization depend on the fractional order β: A smaller β smears the singularities and and a larger β compactifies them to the origin. These are applicable to optical shock waves, filamentation, and phase singularities, as well as to plasma and condensate models in which steep wavefronts develop as a result of nonlinearity versus a competing dispersion. Figure 4 indicates alternating higher and lower levels of infinite amplitude frequency related to disc-type structures in the shape of cotangents. These waveforms represent the extent of localization and high-frequency oscillations in ultrashort pulse propagation when the regime is high-powered. They give an understanding of rogue waves, modulation instability, and self-focusing of beam dynamics and directly provide guidance for designing optical amplifiers, pulse compressers, and nonlinear optical communication systems. Regular solutions represented by sine functions in Figures 5 and 6 show stable bounded regular oscillations that are found in fiber-optics, Bose–Einstein condensates (BECs), and plasma waveguides. The optimal value of the fractional parameter β controls their time evolution: $\beta < 1$ reduces the oscillation frequency and raises the amplitude. Applications of these solutions to optical filtering, periodic pulse trains, and waveguiding systems are also of significance in that the controlled dispersion and memory effects shape the resonance and recovery of signals in these systems. Figures 7 and 8 show a profile of singular solitons that are discontinuous and have sharp spikes, and these profiles greatly depend on the fractional order β. The growth of β strengthens localization and makes singularity occur more easily. The physically relevant applications of such solutions include rogue waves, the dynamics of collapses, and the intense localization of fields in nonlinear dispersion media. They play an important role in ultrafast photonics, supercontinuum generation, and plasma systems, where their role in controlling singularities affects stability and safe signalling. Lastly, Figure 9 represents the modulational instability (MI) gain spectrum $G(\varpi)$ as a function of the perturbation wavenumber, indicating how small perturbations grow and result in the formation of solitons or breathers. The MI curve is bell-shaped, indicating instability bands in which the pump energy transfers efficiently to sidebands. The rainbow color gradient reflects the fractional-order dependence, and demonstrates that by changing β, the instability thresholds can be tuned, allowing the phenomenon to spectrally broaden pulse shapes and produce high-precision shaping.

Physical significance of solution families

The broad family of exact solutions obtained by the ϕ^6-model expansion method possesses diverse physical interpretations in nonlinear optics and plasma physics. The families of solutions $\chi_{1,2}$, $\chi_{5,6}$, $\chi_{29,30}$, $\chi_{31,32}$, $\chi_{33,34}$, $\chi_{37,38}$, $\chi_{39,40}$, $\chi_{49,50}$, $\chi_{51,52}$, and $\chi_{53,54}$ describe nonlinear periodic waves or cnoidal-type wave propagation in a dispersive nonlinear medium. Physically, they are the counterparts of the intensity-modulated continuous waves that can provide precursors to the soliton trains. The families of solutions $\chi_{3,4}$, $\chi_{7,8}$, $\chi_{11,12}$, $\chi_{15,16}$, $\chi_{19,20}$, $\chi_{23,24}$, $\chi_{27,28}$, $\chi_{35,36}$, $\chi_{43,44}$, $\chi_{47,48}$, and $\chi_{55,56}$ represents the solitary localized wave packets in space or time. Bright solitons arise from the solution including $sech(\rho)$, and $csch(\rho)$-type envelopes. Dark solitons will be observed from the solution $tanh(\rho)$. The families of solutions $\chi_{25,26}$, $\chi_{29,30}$, $\chi_{31,32}$, $\chi_{33,34}$, $\chi_{37,38}$, $\chi_{39,40}$, $\chi_{35,36}$, and $\chi_{39,40}$ characterize singular or blow-up nonlinear wave states, which can arise in systems with collapse-type dynamics, higher-order dispersion, or strong nonlinearity. The families of solutions $\chi_{41,42}$, $\chi_{43,44}$, $\chi_{45,46}$, $\chi_{47,48}$, $\chi_{49,50}$, $\chi_{51,52}$, $\chi_{53,54}$, and $\chi_{55,56}$ depict composite nonlinear states that interpolate between solitons and periodic waves. These kinds of forms are frequently linked to nonlinear superpositions that result from breather-type excitations. In every solution, the exponential carrier leads to long-range correlations, anomalous dispersion, and slowed decay, and is particularly significant in complex optical materials, viscoelastic media, and anomalous transport systems. Understanding wave breaking or rogue-wave precursors may benefit from such solutions. These diverse soliton structures open a broad spectrum of physical applications across nonlinear optics, plasma physics, Bose–Einstein condensates, signal processing, optical filtering, and multichannel communication. They also provide models for rogue-wave formation, optical shocks, filamentation, and the mechanisms underlying optical switching and phase-transition dynamics in waveguides or photonic lattices. The Jacobian elliptic and oscillatory solutions correspond to coherent wave patterns with a tunable amplitude and frequency, making them particularly useful for ultrafast optics, periodic pulse train generation, and waveguiding in dispersive media. Moreover, the dependence of these solutions on the fractional parameter β highlights the role of memory effects and nonlocal interactions, which can be finely tuned to control modulational instability thresholds, pulse compression, and nonlinear resonance. These characteristics are directly connected to the physics of ultrafast photonics, supercontinuum generation, modulational instability, and spectral broadening in fiber systems [3]. Collectively, these physical implications demonstrate the versatility of the TFHNLSE framework in modeling and engineering complex wave dynamics in modern nonlinear and dispersive media.

6. Conclusions

The ϕ^6-model expansion method was successfully used in the present paper to examine the exact soliton solutions and their stability in the TFHNLSE. The inclusion of the Caputo fractional derivative facilitates the modeling of memory and hereditary effects, and the TFHNLSE becomes a more realistic, versatile and realistic framework for describing nonlinear wave propagation in complex media like nonlinear optics, as well as quantum fluids. The method of analysis produced a wide class of solitary wave solutions. The ϕ^6-model succeeded in controlling the inherent nonlinearities and the dispersive terms of higher order, which are part and parcel of the TFHNLSE. Stability analysis was performed, and the gain spectrum $G(\varpi)$ quantifies the exponential growth rate of perturbations imposed on a plane wave solution. It has been shown that the interdependence of fractional time derivatives and the high-

order spatial effects plays an exceptional role in determining the soliton's formation, localization, and robustness. However, the study is still constrained by its use of the linear stability framework, the one-dimensional setting, and the Caputo derivative, which might not fully capture the nonlinear or multidimensional dynamics. In order to better describe complex physical scenarios, these limitations point to potential avenues for future research, such as the use of alternative fractional operators, nonlinear stability techniques, and higher-dimensional extensions.

Author contributions

Kanza Noor: Conceptualization, methodology, writing-original draft, formal analysis, investigation, software, validation; Jamshad Ahmad: Resources, supervision, validation, acquisition. All authors have read and approved the final version of the manuscript for publication.

Use of Generative-AI tools declaration

The authors declare they have not used an Artificial Intelligence (AI) tools in the creation of this article.

Conflict of interest

The authors declare that they have no competing interests.

References

1. M. Naber, Time fractional Schrödinger equation, *J. Math. Phys.*, **45** (2004), 3339–3352. https://doi.org/10.1063/1.1769611
2. J. Ahmad, K. Noor, S. Akram, Stability analysis and solitonic behaviour of Schrödinger's nonlinear (2+1) complex conformable time fractional model, *Opt. Quant. Electron.*, **56** (2024), 907. https://doi.org/10.1007/s11082-024-06521-5
3. G. P. Agrawal, Nonlinear fiber optics: Its history and recent progress, *J. Opt. Soc. Am. B*, **28** (2011), A1–A10. https://doi.org/10.1364/JOSAB.28.0000A1
4. P. L. Butzer, U. Westphal, *An introduction to fractional calculus*, In: Applications of fractional calculus in physics, Academic Press, 2000, 1–85. https://doi.org/10.1142/9789812817747_0001
5. M. Nadeem, F. Liu, Y. Alsayaad, Analyzing the dynamical sensitivity and soliton solutions of the time-fractional Schrödinger model with Beta derivative, *Sci. Rep.*, **14** (2024), 8301. https://doi.org/10.1038/s41598-024-58796-z
6. F. Tian, Y. Wang, Z. Li, Numerical simulation of soliton propagation behavior for the fractional-in-space NLSE, *Fractal Fract.*, **8** (2024), 163. https://doi.org/10.3390/fractalfract8040163
7. M. Caputo, Linear models of dissipation whose Q is almost frequency independent, *Ann. Geophys.*, **19** (1966), 383–393. https://doi.org/10.4401/ag-5051

8. K. M. Elhadj, L. Al Sakkaf, U. Al Khawaja, A. Boudjemâa, Singular soliton molecules of the nonlinear Schrödinger equation, *Phys. Rev. E*, **101** (2020), 042221. https://doi.org/10.1103/PhysRevE.101.042221

9. N. I. Okposo, K. Raghavendar, N. Khan, J. F. G. Aguilar, A. M. Jonathan, New exact optical solutions for the Lakshmanan–Porsezian–Daniel equation with parabolic law nonlinearity using the ϕ^6-expansion technique, *Nonlinear Dynam.*, **113** (2025), 4775–4795. https://doi.org/10.1007/s11071-024-10430-3

10. H. U. Rehman, I. Iqbal, M. Mirzazadeh, M. S. Hashemi, A. U. Awan, A, M. Hassan, Optical solitons of new extended (3+1)-dimensional nonlinear Kudryashov's equation via ϕ^6-model expansion method, *Opt. Quant. Electron.*, **56** (2024), 279. https://doi.org/10.1007/s11082-023-05850-1

11. H. X. Jia, D. W. Zuo, Properties of the hybrid solutions for a generalized (3+1)-dimensional KP equation, *Phys. Lett. A*, **525** (2024), 129882. https://doi.org/10.1016/j.physleta.2024.129882

12. X. Zhao, L. Li, F. Yu, Fractional-order effect on soliton solution and the oscillation number for some time-space fractional higher-order nonlinear Schrödinger equations, *Nonlinear Dynam.*, **112** (2024), 13409–13426. https://doi.org/10.1007/s11071-024-09740-3

13. E. A. E. Khazanov, Post-compression of femtosecond laser pulses using self-phase modulation: From kilowatts to petawatts in 40 years, *Quantum Electron.*, **52** (2022), 208. https://doi.org/10.1070/QEL18001

14. A. Sheveleva, U. Andral, B. Kibler, P. Colman, J. M. Dudley, C. Finot, Idealized four-wave mixing dynamics in a nonlinear Schrödinger equation fiber system, *Optica*, **9** (2022), 656–662. https://doi.org/10.1364/OPTICA.445172

15. K. A. Gepreel, R. M. Shohib, M. E. Alngar, Analyzing multiplicative noise effects on stochastic resonant nonlinear Schrödinger equation via two integration algorithms, *Opt. Quant. Electron.*, **57** (2025), 156. https://doi.org/10.1007/s11082-025-08067-6

16. A. Zhang, Y. Zhang, X. Wang, Z. Wang, J. Duan, The stochastic fractional Strichartz estimate and blow-up for Schrödinger equation, 2023. https://doi.org/10.48550/arXiv.2308.10270

17. K. K. Ahmed, H. M. Ahmed, W. B. Rabie, M. F. Shehab, Effect of noise on wave solitons for (3+1)-dimensional nonlinear Schrödinger equation in optical fiber, *Indian J. Phys.*, **98** (2024), 4863–4882. https://doi.org/10.1007/s12648-024-03222-3

18. M. A. S. Murad, M. A. Mustafa, U. Younas, H. Emadifar, A. S. Khalifa, W. W. Mohammed, et al., Soliton solutions to the generalized derivative nonlinear Schrödinger equation under the effect of multiplicative white noise and conformable derivative, *Sci. Rep.*, **15** (2025), 19599. https://doi.org/10.1038/s41598-025-04981-7

19. S. Abbagari, A. Houwe, L. Akinyemi, D. Y. Serge, K. T. Crépin, Multi-hump soliton and rogue waves of the coupled nonlinear Schrödinger equations in a nonlinear left-handed transmission line, *Nonlinear Dynam.*, **113** (2025), 10319–10334. https://doi.org/10.1007/s11071-024-10774-w

20. H. H. Hussein, H. M. Ahmed, S. A. Kandil, W. Alexan, Unveiling diverse solitons in the quintic perturbed Gerdjikov-Ivanov model via a modified extended mapping method, *Sci. Rep.*, **15** (2025), 15881. https://doi.org/10.1038/s41598-025-97981-6

21. W. F. Weng, M. H. Zhang, G. Q. Zhang, Z. Y. Yan, Dynamics of fractional N-soliton solutions with anomalous dispersions of integrable fractional higher-order nonlinear Schrödinger equations, *Chaos*, **32** (2022), 123110. https://doi.org/10.1063/5.0101921

22. M. I. Afridi, T. Islam, M. A. Akbar, M. S. Osman, The investigation of nonlinear time-fractional models in optical fibers and the impact analysis of fractional-order derivatives on solitary waves, *Fractal Fract.*, **8** (2024), 627. https://doi.org/10.3390/fractalfract8110627

23. S. Hussain, G. Arora, R. Kumar, Semi-analytical methods for solving non-linear differential equations: A review, *J. Math. Anal. Appl.*, **531** (2024), 127821. https://doi.org/10.1016/j.jmaa.2023.127821

24. A. Chabchoub, N. P. Hoffman, N. Akhmediev, Modulation instability and New Breathers on finite background, *Phys. Rev. Lett.*, **106** (2011), 204502. https://doi.org/10.1103/PhysRevLett.106.204502

25. M. Onorato, S. Residori, U. Bortolozzo, A. Montina, F. T. Arecchi, Rogue waves and modulational instability in optics and oceanography, *Phys. Rep.*, **528** (2013), 47–89. https://doi.org/10.1016/j.physrep.2013.03.001

26. J. Ahmad, K. Noor, S. Anwar, S. Akram, Stability analysis and soliton solutions of the truncated M-fractional Heisenberg ferromagnetic spin chain model via two analytical methods, *Opt. Quant. Electron.*, **56** (2024), 95. https://doi.org/10.1007/s11082-023-05528-8

27. A. Khare, U. Sukhatme, New periodic and hyperbolic soliton solutions of the nonlinear Schrödinger equation, *J. Math. Phys.*, **43** (2002), 3798–3816.

AIMS Press